Langmuir

Letter

pubs.acs.org/Langmuir

Mass Density and Water Content of Saturated Never-Dried Calcium Silicate Hydrates

Julio C. da Silva,*[,†,∥] Pavel Trtik,[†,‡,§] Ana Diaz,[†] Mirko Holler,[†] Manuel Guizar-Sicairos,[†] Jörg Raabe,[†] Oliver Bunk,[†] and Andreas Menzel*[,†]

[†]Paul Scherrer Institut, Villigen PSI, 5232, Switzerland

[‡]Faculty of Civil Engineering, Czech Technical University in Prague, Prague, 166 36, Czech Republic

[§]Laboratory for Concrete and Construction Chemistry, EMPA, Dübendorf, 8600, Switzerland

Supporting Information

ABSTRACT: Calcium silicate hydrates (C−S−H) are the most abundant hydration products in ordinary Portland cement paste. Yet, despite the critical role they play in determining mechanical and transport properties, there is still a debate about their density and exact composition. Here, the site-specific mass density and composition of C−S−H in hydrated cement paste are determined with nanoscale resolution in a nondestructive approach. We used ptychographic X-ray computed tomography in order to determine spatially resolved mass density and water content of the C−S−H within the microstructure of the cement paste. Our findings indicate that the C−S−H at the border of hydrated alite particles possibly have a higher density than the apparent inner-product C−S−H, which is contrary to the common expectations from previous works on hydrated cement paste.

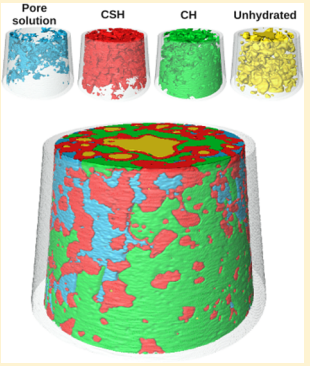

1. INTRODUCTION

Critical to the understanding of cement hydration processes is accurate site-specific knowledge of the mass density of calcium silicate hydrates (C−S−H).[1] For instance, the hypothesis that C−S−H is less dense at the original cement particles' outer rims than in their interior is integral to most modeling of cement-based materials.[2−9] These two types of C−S−H are easily distinguished in electron microscopy and are called inner or outer products, or "phenograins" or "groundmass," respectively.[10]

Density measurements of C−S−H depend on the method of sample preparation and the hydration condition, and various values have been reported.[4−6,8,11−19] Furthermore, most density measurements lack spatial resolution. For site-specific densitometry of C−S−H, we used here ptychographic X-ray computed tomography (PXCT),[20] which is an X-ray imaging technique having demonstrated an isotropic 3D resolution better than 20 nm.[21] PXCT nondestructively provides 3D images of the sample's complex-valued X-ray refractive index, usually written $n(\mathbf{r}) = 1 - \delta(\mathbf{r}) + i\beta(\mathbf{r})$, where the refractive index decrement δ and the absorption index β give rise to phase and absorption contrast, respectively. Having determined δ is often sufficient for density mapping.[22] The high penetration power of X-rays allows for samples of many tens of micrometers in thickness, thus alleviating the risk of altering mass densities when extracting small samples. In a previous study, we could distinguish individual material phases within a 30 μm thick sample of epoxy-impregnated hardened cement paste and determine their densities quantitatively.[23] Here we analyzed more than 400,000 μm^3 of alite-based hardened cement paste in saturated never-dried conditions, corresponding to about 10^9 resolution elements and used accurate measurements of the complex-valued refractive index to gain insight into the composition of the specimen as well.[24,25]

2. EXPERIMENTAL SECTION

Alite powder was put inside a tapering capillary, which was filled with distilled water immediately before both ends were sealed. Sixteen days later, two parts of the capillary were investigated: (i) a small volume of about 25 μm thickness close to the capillary tip, denoted as volume A, and (ii) a larger volume further away from the capillary tip, where the specimen thickness measured about 90 μm, denoted as volume B. Volume B was measured 1 day after volume A. Further details of the sample preparation and the PXCT experiment conducted at the cSAXS beamline of the Swiss Light Source, Villigen, Switzerland, are provided in the Supporting Information.

3. RESULTS AND DISCUSSION

The reconstructed data set of volume A was about 40 × 40 × 23 μm^3 in size with a voxel size of 43.7 nm. Vertical slices of the absorption and phase contrast tomograms are shown in Figure 1. The 3D spatial resolution of the phase contrast images was

Received: November 16, 2014
Revised: January 23, 2015
Published: March 20, 2015

DOI: 10.1021/la504478j
Langmuir 2015, 31, 3779−3783

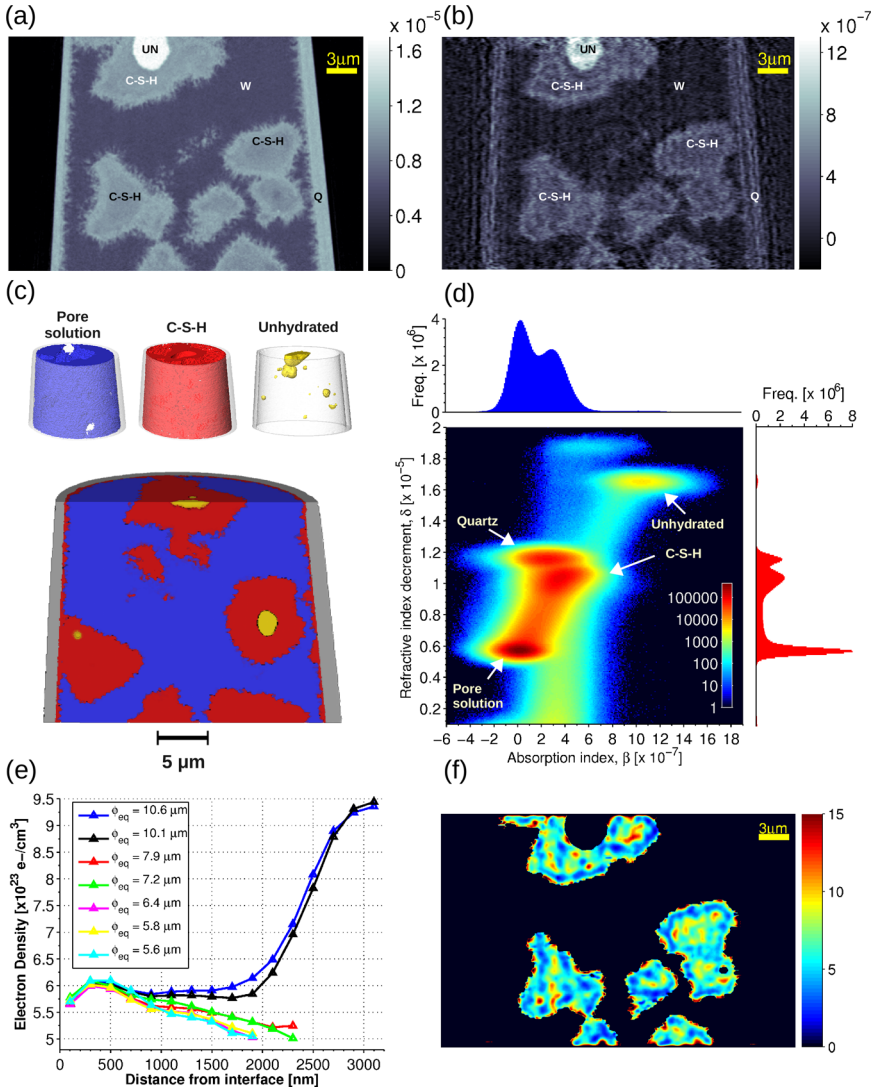

Figure 1. Vertical slices of the (a) phase contrast and (b) absorption tomograms of the hydrated cement paste in the volume A, where the colorbars correspond to δ and β, respectively. UN: Unhydrated C_3S; C−S−H: calcium silicate hydrate; Q: quartz capillary; and W: pore solution. (c) 3D renderings of the volume showing how the material phases are located with respect to each other. (d) Bivariate histogram of δ and β. (e) Radial electron density profile of the particles as a function of distance from surface inward. The effective particle diameters are shown in the legend. (f) Site-specific water content of the C−S−H at the same slice shown in (a) and (b) with a resolution of 1 μm, where the colorbar is given in units of mol of water.

estimated to be 130 nm, whereas the resolution of the absorption images was found to be 250 nm due to lower signal-to-noise ratio. As was seen as well in environmental scanning electron microscopy,[26] C−S−H needle-like structures, hundreds of nanometers in length, growing outward from the surfaces of the original particles were characteristic for the morphology of the hydrated alite particles.

To identify the material phases from the 3D images from volume A, threshold-based image segmentation was carried out on the phase contrast images in a similar way as presented before.[23] We identified the C−S−H, the capillary pores, which represent the part of the gross volume that has not been filled by the products of the hydration, and a few unhydrated residues of C_3S. No CH was found, and gel pores, i.e., interconnected interstitial spaces within the C−S−H structure that are much smaller than the capillary pores, were not spatially resolved. The 3D renderings of the volume are presented in Figure 1c. Thirteen individual loosely packed C_3S particles could be identified, seven of which were fully contained within the tomographic field of view. Two out of these seven were only partially hydrated and contained some residual unhydrated C_3S. The other five were fully hydrated. The bivariate histogram of the refractive index decrement δ and absorption index β values extracted from the tomograms is shown in Figure 1d.

For the characterization of the volume B, the reconstructed data set size was about $110 \times 110 \times 68$ μm^3 with identical voxel size of 43.7 nm. Vertical slices of the absorption and phase contrast tomograms are displayed in Figure 2. The 3D spatial resolution obtained on the phase contrast images was approximately 130 nm, while the absorption images had resolution of about 200 nm. The identified material phases are C−S−H, CH, unhydrated residues of C_3S, and capillary pores, which were much less abundant than in volume A. Here too, gel pores were not resolved. Figure 2c displays how the phases are located with respect to each other, and Figure 2d displays the bivariate histogram of δ and β. The combined use of absorption and phase information facilitates the identification

DOI: 10.1021/la504478j
Langmuir 2015, 31, 3779−3783

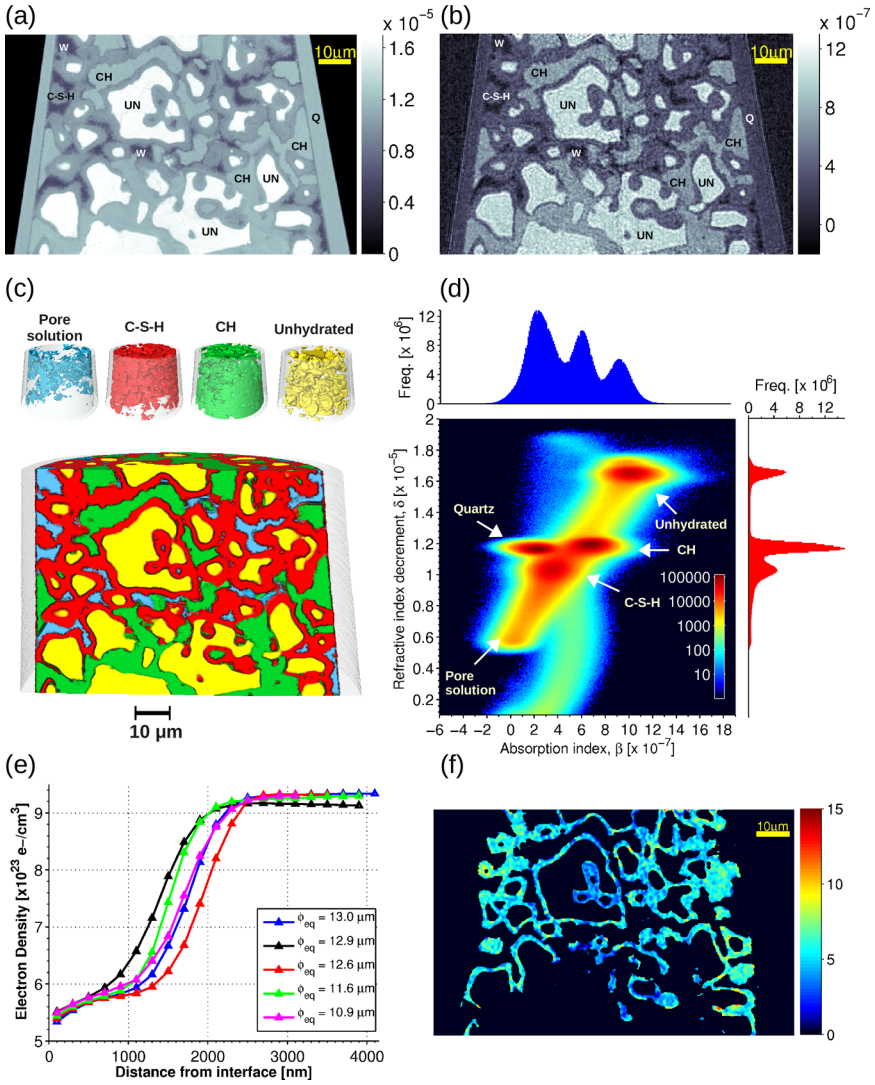

Figure 2. Vertical slices of the (a) phase contrast and (b) absorption tomograms of the hydrated cement paste in the volume B, where the colorbars correspond to δ and β, respectively. UN: Unhydrated C_3S; CH: calcium hydroxide; C−S−H: calcium silicate hydrate; Q: quartz capillary; and W: pore solution. (c) 3D renderings of the volume showing how the material phases are located with respect to each other. (d) Bivariate histogram of δ and β. (e) Radial electron density profile of the particles as a function of distance from surface inward. The effective particle diameters are shown in the legend. (f) Site-specific water content of the C−S−H at the same slice shown in (a) and (b) with a resolution of 1 μm, where the colorbar is given in units of mol of water.

of different material phases independent of sample morphology, which is often challenging for automated segmentation.

Segmentation of individual particles, as detailed in the Supporting Information, allows for the electron density within each particle to be measured as a function of the distance from the surface. Such electron density profiles are displayed in Figures 1e and 2e for volumes A and B, respectively. All seven particles found to be fully contained in volume A were evaluated, whereas only five loosely packed particles without apparent concavities from volume B were used because of the challenging task of distinguishing the particles boundaries as described in the Supporting Information. For fully hydrated particles, the highest value of electron density was found between approximately 200 and 600 nm from the apparent particle surface. Further toward the center of the particles, the electron density decreases. Contrary to what has been hitherto hypothesized,[4−6,8] this indicates that the C−S−H at the border can have a higher density than the inner-product C−S−H.

In the case of partially hydrated particles, we observe a different trend. Close to the surface, the partially hydrated particles in volume A exhibit similar electron densities as the fully hydrated particles, leveling off further from the boundary before increasing to the expected value for unhydrated C_3S. A similar behavior is observed in volume B. However, the shell of C−S−H around the unhydrated cores was found to be significantly thinner. This difference can also be observed on the bivariate histograms. Whereas in Figure 2d (volume B) C−S−H occupies a region fairly symmetric in both δ and β, the C−S−H distribution in Figure 1d (volume A) appears "skewed" and comprises higher values of both δ and β. This indicates the presence of two types of C−S−H in volume A not thus observed in volume B. Since the particles in volume A were in constant contact with water and the local water-to-solid ratio in volume A was significantly higher than for the rest of the sample (cf. Figure 1c), we consider volume B much more representative of realistic alite-based cement paste. Whereas CH was not found in volume A, in volume B it limits the

DOI: 10.1021/la504478j
Langmuir 2015, 31, 3779−3783

Table 1. Average Mass Density Values and Composition of the C−S−H in the Fully and Partially Hydrated Particles, Where y Represents the Estimated Number of Moles of Water in the Stoichiometry of C−S−H, Which Is Written As $C_{1.75}SH_y$

C−S−H	mass density [g·cm^{-3}]	relative mass of C	relative mass of S	relative mass of H	number of moles of water (y)
fully hydrated particles in volume A	1.726 ± 0.006[a]	0.334 ± 0.009[a]	0.204 ± 0.006[a]	0.462 ± 0.014[a]	7.5 ± 0.4[a]
	1.909 ± 0.005[b]	0.420 ± 0.009[b]	0.257 ± 0.006[b]	0.324 ± 0.015[b]	4.2 ± 0.3[b]
partially hydrated particles in volume A	1.860 ± 0.004[a]	0.383 ± 0.007[a]	0.235 ± 0.004[a]	0.382 ± 0.011[a]	5.4 ± 0.3[a]
	1.96 ± 0.04[b]	0.387 ± 0.011[b]	0.237 ± 0.007[b]	0.376 ± 0.018[b]	5.3 ± 0.4[b]
partially hydrated particles in volume B	1.828 ± 0.005	0.389 ± 0.010	0.238 ± 0.006	0.373 ± 0.015	5.2 ± 0.4

[a]Apparent inner-product C−S−H. [b]Apparent outer-product C−S−H.

availability of pore solution for hydration by restricting the space around the particles and thus may slow down the hydration process.

These findings corroborate the observation by Muller et al.[19] that C−S−H density depends on hydration. Moreover, since we did not resolve the gel porosity, there is significant uncertainty on account of the unknown contribution of interlayer water to our density measurements. With regard to the high-density C−S−H found in fully hydrated particles from volume A, we speculate that this is related to water diffusion. As the C_3S particles get hydrated, the water could diffuse inward while the outer products could be pushed outward, which has possibly caused the increase of density on the border of the fully hydrated particle in volume A.

In order to assess in more detail the site-specific water content of C−S−H in our measurements, we analyzed its stoichiometry C_xSH_y, where x and y remain to be determined. For the analysis, we assume x = 1.75 because the number of moles of C should not vary far from this value according to the literature.[8,15,18,27,28] Under this assumption and utilizing the information on the complex-valued refractive index as provided by PXCT, the water content of C−S−H can be quantified as further described in the Supporting Information. Mean values of mass density and composition of the C−S−H are presented in Table 1.

The values of C−S−H densities presented here are higher than those deduced from our previous measurements of epoxy-impregnated hardened cement paste,[23] which seems to confirm the hypothesis stated therein that the results may have been affected by incomplete epoxy resin impregnation of gel porosity and carbonation-induced decalcification. Since the gel pores contain water below the spatial resolution of the images, the measured mass density of C−S−H is lower with higher degrees of hydration.

Extracted molar concentration of water in the C−S−H of the hydrated particles is shown in Figures 1f and 2f. We observed that the fully hydrated particles of volume A exhibit a higher amount of water at the particle border than in the inner part. It is generally assumed that this water is located in the gel pores, which are more present in the inner part. This also corroborates the separation of high-density C−S−H at the border and low-density C−S−H in the inner part. A similar behavior was observed in the partially hydrated particles of volume A but with less difference between inner and outer parts. Although we did not observe the same behavior in the partially hydrated particles of volume B, Figure 2f indicates a lower water content of the C−S−H material in the center of the capillary.

4. CONCLUSIONS

In conclusion, we measured the density and water content of C−S−H in ∼16-day old saturated never-dried cement paste using PXCT. The density values of such C−S−H ranges from 1.726 g·cm^{-3} to 1.96 g·cm^{-3}, and its water content ranges from 4.3 to 7.6 mol, assuming a C/S molar ratio of 1.75. Within individual alite particles, we observed that the C−S−H density can depend on the particles' states of hydration. For the fully hydrated particles, the estimated density of the outer-product C−S−H was larger than that of the inner-product C−S−H, whereas for the partially hydrated particles, the densities of the apparent outer and the inner products hardly differed. These results exemplify new measurement opportunities at the nanoscale for a large variety of complex multiphase systems.

■ ASSOCIATED CONTENT

Supporting Information

Further experimental details and methods, supplemental tables and figures. This material is available free of charge via the Internet at http://pubs.acs.org.

■ AUTHOR INFORMATION

Corresponding Authors

*E-mail: jdasilva@esrf.fr.
*E-mail: andreas.menzel@psi.ch.

Present Address

[‖]European Synchrotron Radiation Facility, Grenoble, 38000, France.

Notes

The authors declare no competing financial interest.

■ ACKNOWLEDGMENTS

We would like to kindly thank Dr. S. Bergold (University of Erlangen, Germany) for providing the sample of alite powder, and X. Donath for excellent technical support during the X-ray experiments at the beamline. We also thank the Swiss National Science Foundation SNF for the support to the work of J. C. da Silva (Grant No. 137772). Instrumentation development was supported by SNF (R'EQUIP, No. 145056, "OMNY") and the Competence Centre for Materials Science and Technology (CCMX) of the ETH-Board, Switzerland.

■ REFERENCES

(1) Calcium silicate hydrate is written C−S−H in accordance with the conventional cement chemistry notation (C = CaO, S = SiO_2, H = H_2O) defined in Taylor, H. F. W. *Cement Chemistry*; Thomas Thelford Publishing: London, 1997.

(2) van Breugel, K. *Simulation of Hydration and Formation of Structure in Hardening Cement-Based Materials*. PhD Thesis, TU Delft, November, 1991.

(3) van Breugel, K.; Koenders, E. A. B. Numerical Simulation of Hydration-Driven Moisture Transport in Bulk and Interface Paste in Hardening Concrete. *Cem. Concr. Res.* **2000**, *30*, 1911−1914.

(4) Tennis, P. D.; Jennings, H. M. A Model for Two Types of Calcium Silicate Hydrate in the Microstructure of Portland Cement Pastes. *Cem. Concr. Res.* **2000**, *30*, 855−863.

DOI: 10.1021/la504478j
Langmuir 2015, 31, 3779−3783

(5) Jennings, H. M. Colloid Model of C−S−H and Implications to the Problem of Creep and Shrinkage. *Mater. Struct.* **2004**, *37*, 59−70.
(6) Constantinides, G.; Ulm, F.-J. The Nanogranular Nature of C−S−H. *J. Mech. Phys. Solids* **2007**, *55*, 64−90.
(7) van Mier, J. G. M. Multi-Scale Interaction Potentials (F − r) for Describing Fracture of Brittle Disordered Materials like Cement and Concrete. *Int. J. Fract.* **2007**, *143*, 41−78.
(8) Jennings, H. M. Refinements to Colloid Model of C−S−H in Cement: CM-II. *Cem. Concr. Res.* **2008**, *38*, 275−289.
(9) Dolado, J. S.; van Breugel, K. Recent Advances in Modeling for Cementitious Materials. *Cem. Concr. Res.* **2011**, *41*, 711−726.
(10) Diamond, S.; Bonen, D. Microstructure of Hardened Cement Paste − A New Interpretation. *J. Am. Ceram. Soc.* **1993**, *76*, 2993−2999.
(11) Powers, T. C.; Brownyard, T. L. Studies of the Physical Properties of Hardened Portland Cement Paste. *J. Am. Concr. Inst. (Proc.)* **1947**, *43*, 669−712.
(12) Brunauer, S.; Kantro, D. L.; Copeland, L. E. The Stoichiometry of the Hydration of *β*-Dicalcium Silicate and Tricalcium Silicate at Room Temperature. *J. Am. Chem. Soc.* **1958**, *80*, 761−767.
(13) Feldman, R. F. Helium Flow and Density Measurement of the Hydrated Tricalcium Silicate−Water System. *Cem. Concr. Res.* **1972**, *2*, 123−136.
(14) Goto, S.; Daimon, M.; Hosaka, G.; Kondo, R. Composition and Morphology of Hydrated Tricalcium Silicate. *J. Am. Ceram. Soc.* **1976**, *59*, 281−284.
(15) Rayment, D. L.; Majumdar, A. J. The Composition of the C−S−H Phases in Portland Cement Pastes. *Cem. Concr. Res.* **1982**, *12*, 753−764.
(16) Young, J. F.; Hansen, W. Volume Relationships for C−S−H Formation Based on Hydration Stoichiometries. *Mater. Res. Soc. Symp. Proc.* **1987**, *85*, 313−322.
(17) Brouwers, H. J. H. The Work of Powers and Brownyard Revisited: Composition of Portland Cement Paste. *Cem. Concr. Res.* **2004**, *34*, 1697−1716.
(18) Allen, A. J.; Thomas, J. J.; Jennings, H. M. Composition and Density of Nanoscale Calcium−Silicate−Hydrate in Cement. *Nat. Mater.* **2007**, *6*, 311−316.
(19) Muller, A. C. A.; Scrivener, K. L.; Gajewicz, A. M.; McDonald, P. J. Densification of C−S−H Measured by ^{1}H NMR Relaxometry. *J. Phys. Chem. C* **2013**, *117*, 403.
(20) Dierolf, M.; Menzel, A.; Thibault, P.; Schneider, P.; Kewish, C. M.; Wepf, R.; Bunk, O.; Pfeiffer, F. Ptychographic X-ray Computed Tomography at the Nanoscale. *Nature* **2010**, *467*, 436−439.
(21) Holler, M.; Diaz, A.; Guizar-Sicairos, M.; Karvinen, P.; Färm, E.; Härkönen, E.; Ritala, M.; Menzel, A.; Raabe, J.; Bunk, O. X-ray Ptychographic Computed Tomography at 16 nm Isotropic 3D Resolution. *Sci. Rep.* **2014**, *4*, 3857.
(22) Diaz, A.; Trtik, P.; Guizar-Sicairos, M.; Menzel, A.; Thibault, P.; Bunk, O. Quantitative X-ray Phase Nanotomography. *Phys. Rev. B: Condens. Matter Mater. Phys.* **2012**, *85*, 020104(R).
(23) Trtik, P.; Diaz, A.; Guizar-Sicairos, M.; Menzel, A.; Bunk, O. Density Mapping of Hardened Cement Paste Using Ptychographic X-ray Computed Tomography. *Cem. Concr. Compos.* **2013**, *36*, 71−77.
(24) Clark, J. N.; Putkunz, C. T.; Pfeifer, M. A.; Peele, A. G.; Williams, G. J.; Chen, B.; Nugent, K. A.; Hall, C.; Fullagar, W.; Kim, S.; McNulty, I. Use of a Complex Constraint in Coherent Diffractive Imaging. *Opt. Express* **2010**, *18*, 1981−1993.
(25) Yan, H.; Chu, Y. S.; Maser, J.; Nazaretski, E.; Kim, J.; Kang, H. C.; Lombardo, J. J.; Chiu, W. K. S. Quantitative X-ray Phase Imaging at the Nanoscale by Multilayer Laue Lenses. *Sci. Rep.* **2013**, *3*, 1307.
(26) Möser, B.; Stark, J. A New Model of Ordinary Portland Cement Hydration Derived by Means of ESEM-FEG. In *Materials Science of Concrete: Cement and Concrete - Trends and Challenges*; Boyd, A., Mindess, S., Skalny, J., Eds.; The American Ceramic Society: Westerville, OH, 2002; pp 89−107.
(27) Thomas, J. J.; Jennings, H. M.; Allen, A. J. Relationships between Composition and Density of Tobermorite, Jennite, and Nanoscale CaO−SiO_2−H_2O. *J. Phys. Chem. C* **2010**, *114*, 7594−7601.
(28) Richardson, I. G. The Nature of C−S−H in Hardened Cements. *Cem. Concr. Res.* **1999**, *29*, 1131−1147.

NOTE ADDED AFTER ASAP PUBLICATION

This article was published ASAP on March 26, 2015. Panel (d) in Figure 1 and panel (d) in Figure 2 have been corrected. The correct version was published on April 7, 2015.

DOI: 10.1021/la504478j
Langmuir 2015, 31, 3779−3783